

Article

# Grindability of Ti–Nb–Cu Alloys for Dental Machining Applications

Masatoshi Takahashi <sup>1,\*</sup> , Masafumi Kikuchi <sup>2</sup>  and Yukyo Takada <sup>1</sup>

<sup>1</sup> Division of Dental Biomaterials, Tohoku University Graduate School of Dentistry, 4-1 Seiryomachi, Aoba-ku, Sendai 980-8575, Japan; yukyo.takada.a1@tohoku.ac.jp

<sup>2</sup> Department of Biomaterials Science, Kagoshima University Graduate School of Medical and Dental Sciences, 8-35-1 Sakuragaoka, Kagoshima 890-8544, Japan; kikuchi@dent.kagoshima-u.ac.jp

\* Correspondence: takahashi@m.tohoku.ac.jp; Tel.: +81-22-717-8317

**Abstract:** We developed high-strength Ti–Nb–Cu alloys and investigated their grindability. The grindability of each alloy was evaluated based on the volume of metal removed per minute (grinding rate) and on the ratio of the metal volume removed to the volume of the wheel material lost (grinding ratio). The grinding rate of the Ti-6%Nb-4%Cu, Ti-18%Nb-2%Cu, and Ti-24%Nb-1%Cu alloys significantly exceeded that of unalloyed titanium at high, medium, and low grinding speeds, respectively. Additionally, the Ti-6%Nb-4%Cu alloy exhibited an excellent grinding ratio. Generally, materials with high strength and hardness frequently exhibit poor machinability; however, the Ti–Nb–Cu alloys developed in our study presented favorable grindability characteristics and, therefore, demonstrated good potential for application as dental titanium alloys that can be subjected to computer-aided design/manufacturing processes.

**Keywords:** grinding rate; grinding ratio; titanium alloy; computer-aided design/manufacturing; dental alloy; abrasive cutting



**Citation:** Takahashi, M.; Kikuchi, M.; Takada, Y. Grindability of Ti–Nb–Cu Alloys for Dental Machining Applications. *Metals* **2022**, *12*, 861. <https://doi.org/10.3390/met12050861>

Academic Editor: Asit Kumar Gain

Received: 13 April 2022

Accepted: 15 May 2022

Published: 18 May 2022

**Publisher's Note:** MDPI stays neutral with regard to jurisdictional claims in published maps and institutional affiliations.



**Copyright:** © 2022 by the authors. Licensee MDPI, Basel, Switzerland. This article is an open access article distributed under the terms and conditions of the Creative Commons Attribution (CC BY) license (<https://creativecommons.org/licenses/by/4.0/>).

## 1. Introduction

Owing to its excellent biocompatibility and good corrosion resistance, titanium is a suitable biomaterial for dental implants and denture frameworks, and its clinical applications include the fabrication of cast crowns. However, titanium exhibits poor machinability (ease of cutting) [1–3] that prolongs its manipulation time (processing, occlusal adjustment, and final polishing) and often results in a short tool life. Consequently, the manufacturing cost of titanium dental prostheses is extremely high. In recent years, computer-aided design/manufacturing (CAD/CAM) processes have been increasingly applied in the designing and milling of dental prostheses composed of zirconia, glass ceramics, and hybrid composite resins. Despite the poor machinability of titanium, milling titanium prostheses using CAD/CAM technology would be beneficial because the high melting point and reactivity of titanium at high temperatures are intrinsic properties that incidentally pose a challenge to the use of casting or additive manufacturing [4]. Improving the machinability of titanium would reduce the cost of fabricating titanium prostheses using dental CAD/CAM milling. Improving key aspects of fabrication, such as machining accuracy, ease of manual occlusal adjustment, and final polishing of the prosthesis, can significantly expand the range of dental applications of titanium alloys.

Various binary titanium alloys have been developed, and their grindability (ease of abrasive cutting) has been tested using a dental carborundum wheel [5–11]. Certain alloy compositions including Ti–Ag, Ti–Cu, Ti–Nb, Ti–Zr, and Ti–Cr have demonstrated excellent grindability rates (volume of metal ground per minute) despite their hardness and strength properties surpassing those of titanium [5–7]. Alloys with favorable grindability features are also known to demonstrate decreased elongation and the existence of secondary phases, such as intermetallic compounds Ti<sub>2</sub>Ag and Ti<sub>2</sub>Cu or an omega ( $\omega$ )

phase. Such precipitated secondary phases possibly act as local brittle zones, similar to the free-machining additives in free-machining alloys [12]. This claim is further supported by the fact that titanium alloys with a single  $\alpha$  phase and no secondary phases (e.g., Ti-Hf) do not exhibit significant improvements in the grindability despite their decreased elongation performance [8].

Among the titanium alloys with improved grindability, the volume of Ti-30 mass%Nb (hereafter, “%” stands for “mass%”) alloy ground at slow grinding speeds (500 and 750 m/min) for 1 min was double that of unalloyed titanium at the same grinding speed [5]. At grinding speeds of 1000 m/min and above, the volume of the ground Ti-30%Nb alloy was equal to that of titanium. In addition, the volume of the ground Ti-5%Cu alloy was significantly higher than that of titanium at a grinding speed of 750 m/min or more [5]. The positive change (improvement) was significantly greater at higher speeds. The volume of the Ti-5%Cu alloy ground at 1500 m/min was 2.4 times higher than that of titanium. However, the speed-dependence of the grindability improvements for different alloys has not yet been fully understood. By combining these alloys, it may be possible to achieve excellent grindability at both low and high speeds. In view of the above, we focused on using Nb and Cu as alloying elements for titanium.

A previous study investigated the mechanical properties of ternary Ti–Nb–Cu alloys [13], such as 6%Nb-4%Cu, 18%Nb-2%Cu, and 24%Nb-1%Cu, reporting tensile strengths of 700 MPa or higher. These values exceeded those of base binary titanium alloys; in particular, the strength of Ti-18%Nb-2%Cu exceeded 800 MPa. Moreover, the average elongation of these alloys was approximately 4%, and their mechanical properties satisfied the ISO 22674 criteria for type-four metallic materials [14]. Based on these findings, the studied ternary Ti–Nb–Cu alloys were deemed suitable for use in high load-bearing dental applications. Notably, the alloy phases were  $\alpha$  for Ti-6%Nb-4%Cu,  $\alpha + \beta$  for Ti-18%Nb-2%Cu, and  $\alpha + \beta$  (near  $\beta$ ) for Ti-24%Nb-1%Cu. Thus, the alloy phases of Ti–Nb–Cu alloys, except Ti-6%Nb-4%Cu, were not single  $\alpha$  phases and demonstrated less elongation compared with titanium. These alloys could potentially exhibit excellent grindability, although it is generally stated that materials with high strength and hardness exhibit poor machinability. Therefore, this study investigated the grindability of the Ti–Nb–Cu alloys.

## 2. Materials and Methods

### 2.1. Preparation of Specimens

The following alloy compositions were prepared and tested in this study: Ti-6%Nb-4%Cu (6Nb4Cu), Ti-18%Nb-2%Cu (18Nb2Cu), and Ti-24%Nb-1%Cu (24Nb1Cu). Our method drew from previous studies [5,6,13]. The desired amounts of Ti sponge (>99.8%, grade S-90, Osaka Titanium Technologies, Amagasaki, Japan), Nb (>99.9%, H.C. Starck, Goslar, Germany), and Cu (>99.99%, The Research Institute for Electric and Magnetic Materials, Sendai, Japan) were melted in an arc melting furnace (TAM-4S, Tachibana Riko, Sendai, Japan) to form a 15 g ingot for each alloy.

To make a casting mold, a plate-wax pattern (3.5 mm  $\times$  8.5 mm  $\times$  30.5 mm) was invested in a casting ring (outer diameter 38 mm, inner diameter 35 mm, and length 55 mm) with a magnesia-based investment material (Selevest CB, Selec, Osaka, Japan). The molds were then heated in an electric furnace following the manufacturer’s instructions. The ingots of each Ti–Nb–Cu alloy were cast into the molds within an argon gas-pressure dental titanium casting machine (Castmatic-S, Iwatani, Osaka, Japan) at the mold temperature of 200 °C. Subsequently, the samples were bench-cooled to room temperature and then removed from the mold material. Prior to testing, all the surfaces (approximately 250  $\mu$ m at layer width) for each casting were ground using 180–800 grit SiC paper to eliminate the hardened surface layer (reaction layer with the investment material). The thickness of the hardened surface layer of dental titanium castings was reported to be 150–200  $\mu$ m [4]. Three specimens with dimensions of 3.0 mm  $\times$  8.0 mm  $\times$  30 mm were fabricated for each type of alloy.

## 2.2. X-ray Diffractometry

X-ray diffraction (XRD) was performed using Cu-K $\alpha$  radiation, generated at 30 kV and 10 mA, and an X-ray diffractometer (D2 PHASER, Bruker AXS, Tokyo, Japan). Measurements were carried out over a  $2\theta$  range of 30–90°, with a scanning step width of 0.03°. The Crystallography Open Database was used for phase identification.

## 2.3. Hardness Tests

The Vickers hardness of the specimens was determined using a micro Vickers hardness tester (HM-102, Mitutoyo, Kawasaki, Japan) under a load of 1.961 N and dwell time of 30 s. The tests ( $n = 9$ ) were conducted at three randomly selected points for each specimen. The results were statistically analyzed with a statistical software (IBM SPSS Statistics version 28, IBM Japan, Tokyo, Japan) using one-way analysis of variance (ANOVA) and Tukey's honestly significant difference (HSD) tests at a significance level of  $\alpha = 0.05$ .

## 2.4. Grinding Test

A carborundum wheel (#4: diameter 15.8 mm, thickness 1.6 mm, Shofu, Kyoto, Japan) fitted onto an electric dental handpiece (LM-I, GC, Tokyo, Japan) was used to grind the alloy specimens, as in previous studies [5–7]. A 3.0 mm thick cross-section of the specimens was ground for 1 min at 0.98 N and at one of the following five circumferential speeds: 500, 750, 1000, 1250, or 1500 m/min.

The grindability performance of the alloys was evaluated based on the volume of metal removed per minute (grinding rate) and on the ratio of the metal volume removed to the volume of the wheel material lost (grinding ratio). The volume of the wheel material lost was determined according to the decrease in the wheel diameter. Generally, the grinding rate and ratio affect the processing time and tool life, respectively. The test was performed twice for each specimen at each grinding speed. A new wheel was used for each test. The results ( $n = 6$ ) were also statistically analyzed using one-way ANOVA and Tukey's HSD test at a significance level of  $\alpha = 0.05$ . After the grinding test was performed, the metal chips, surface of the wheel, and ground surfaces of the metal specimens were observed using a scanning electron microscope equipped with energy dispersive X-ray spectroscopy (EDS) (JSM-6060, JEOL, Tokyo, Japan). The particles that adhered to the wheel after the test and the ground surfaces were analyzed with EDS. For comparison, the metal chips, wheel surfaces, and ground surfaces of titanium (Ti) obtained in a previous study were also observed under the same conditions as those for Ti–Nb–Cu.

# 3. Results

## 3.1. X-ray Diffractometry

The XRD patterns of the Ti–Nb–Cu alloys used in this study are depicted in Figure 1. The peaks in the XRD pattern of 6Nb4Cu primarily matched those of the  $\alpha$  phase (hexagonal close-packed). Peaks corresponding to Ti<sub>2</sub>Cu were observed, albeit with a weak intensity. The peaks in the spectrum of the 18Nb2Cu alloy matched the characteristic peaks of the  $\alpha$  and  $\beta$  phases (body-centered cubic). The intensities of the  $\alpha$ -related peaks were high, whereas those of the  $\beta$ -related peaks were low. The peaks of the 24Nb1Cu alloy primarily matched those of the  $\beta$  phase. Other phases such as the  $\alpha''$  phase (orthorhombic) and metastable  $\omega$  phase (hexagonal) were also present.

## 3.2. Hardness

The Vickers hardness values of the Ti–Nb–Cu alloys are illustrated in Figure 2. Similar data for titanium obtained from a previous study [15] are also presented for comparison. The hardness results for the different Ti–Nb–Cu alloys significantly exceeded that of Ti ( $p < 0.01$ ). The hardness values of the 6Nb4Cu, 18Nb2Cu, and 24Nb1Cu alloys were 260, 328, and 377, respectively, demonstrating significant divergence ( $p < 0.01$ ).

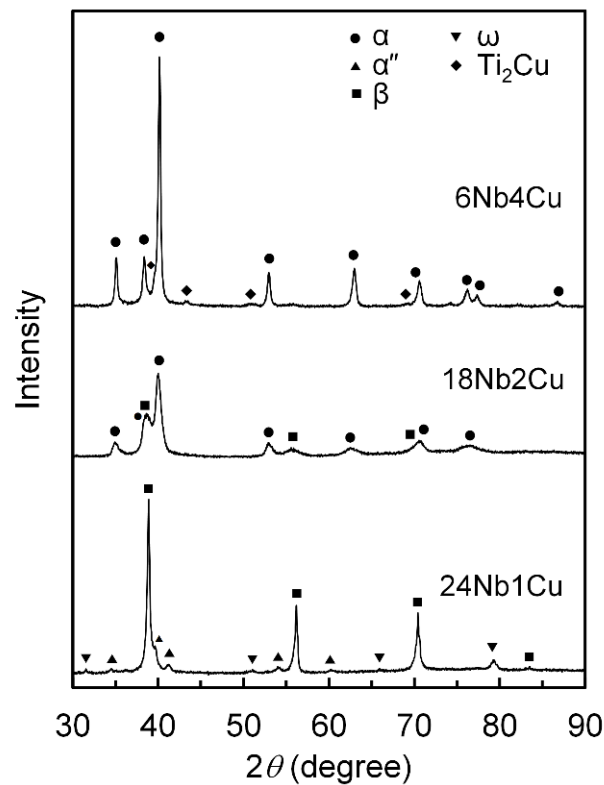


Figure 1. X-ray diffraction patterns obtained from Ti–Nb–Cu alloys.

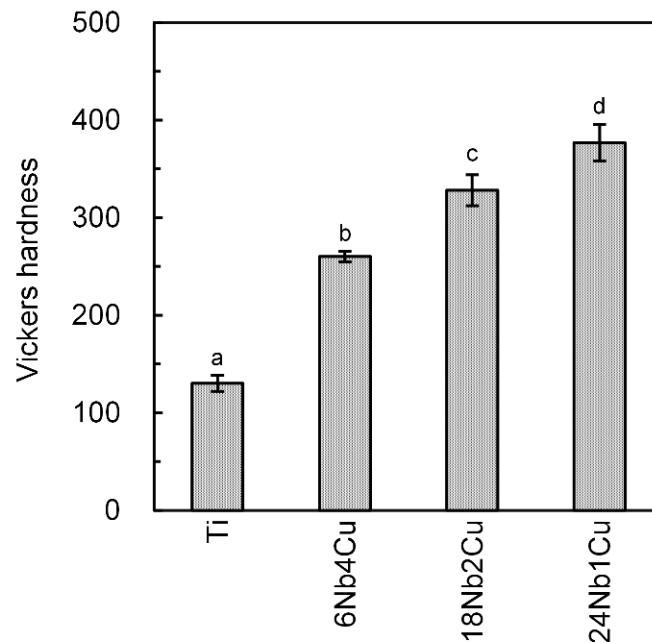
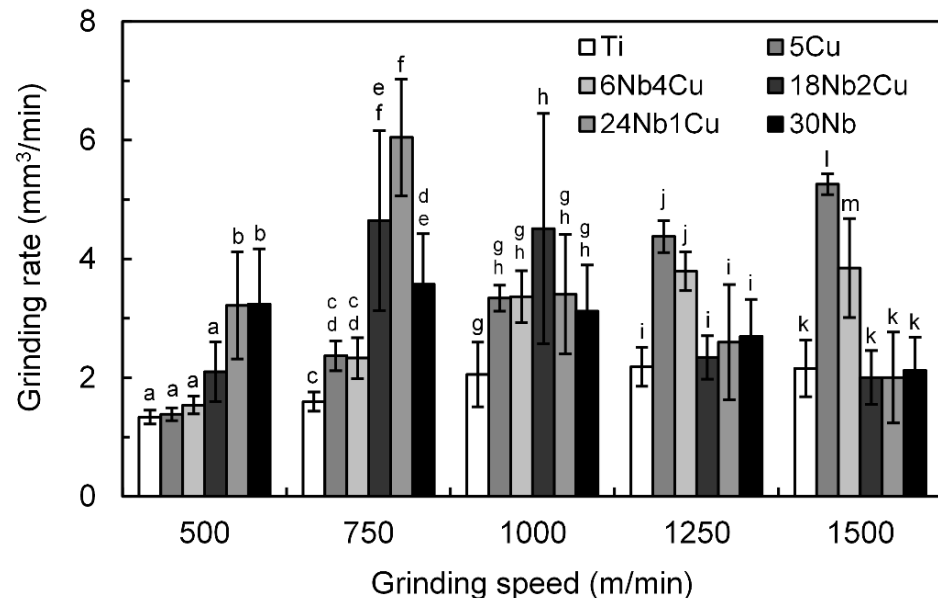


Figure 2. Vickers hardness values for Ti–Nb–Cu alloys. Different roman letters indicate a statistically significant difference ( $p < 0.05$ ).

### 3.3. Grindability

The grinding rates of the Ti–Nb–Cu alloys at five different grinding speeds are depicted in Figure 3. The data for Ti, Ti-5%Cu (5Cu), and Ti-30%Nb (30Nb) obtained in previous studies are also included for comparison [5,6]. The grinding rates of the Ti–Nb–Cu alloys tended to increase with the Nb concentration, within the range of 500–750 m/min. Remarkably, at 500 m/min, the grinding rate for 24Nb1Cu was significantly higher ( $p < 0.001$ ) and 2.4 times larger than that of titanium. The grinding rates for

18Nb2Cu and 24Nb1Cu at 750 m/min were significantly higher ( $p < 0.001$ ) and 2.9 and 3.8 times larger than that of titanium, respectively. The grinding rate for 18Nb2Cu at 1000 m/min was significantly higher ( $p < 0.01$ ) and 2.2 times larger than that of titanium. The grinding rates for 6Nb4Cu and 24Nb1Cu at 1000 m/min were also higher than that of Ti, although the difference was not statistically significant. The grinding rate for 6Nb4Cu significantly surpassed ( $p < 0.001$ ) that of titanium at 1250 m/min and above. The corresponding grinding rates for 6Nb4Cu at 1250 and 1500 m/min were 1.7 times and 1.8 times higher than those of Ti, respectively.

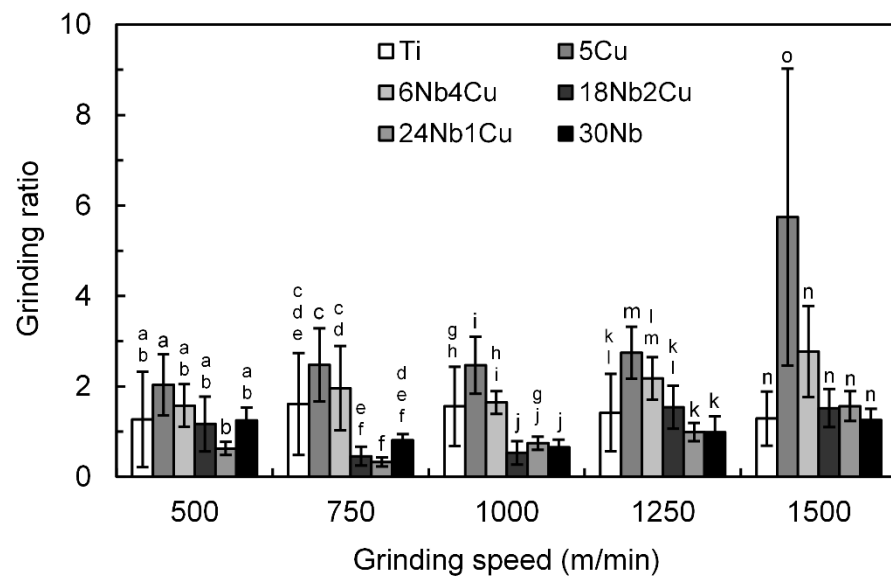


**Figure 3.** Grinding rates for Ti–Nb–Cu alloys. At a particular grinding speed, identical roman letters indicate a statistically insignificant difference ( $p > 0.05$ ) between the grinding rates for titanium and the alloy, whereas different letters indicate a statistically significant difference.

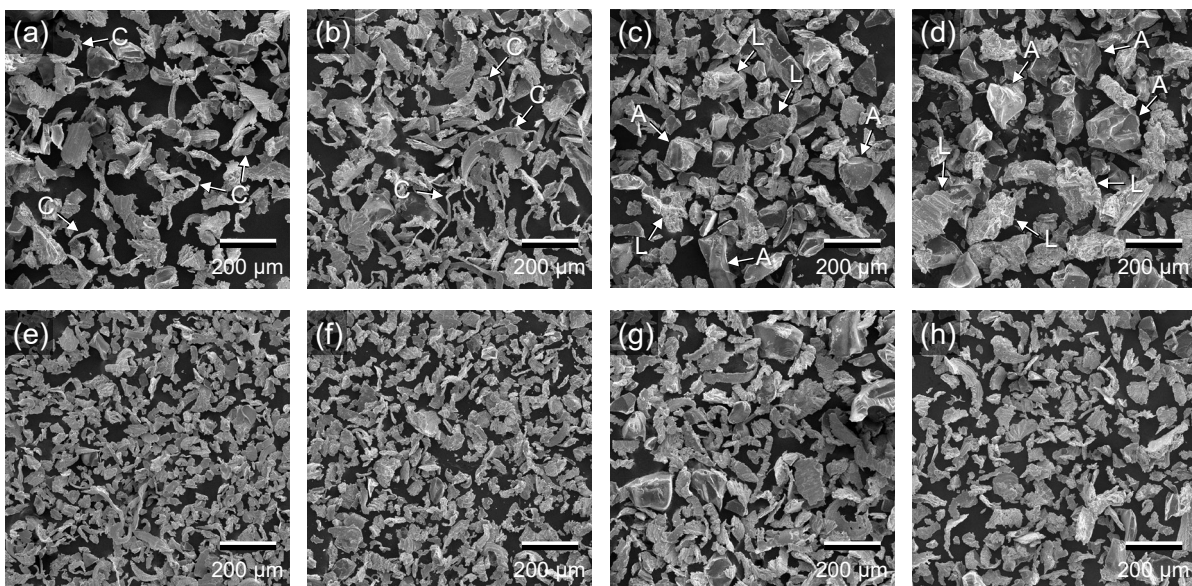
The grinding ratios of the Ti–Nb–Cu alloys at five different grinding speeds are illustrated in Figure 4. Relevant data for Ti, 5Cu, and 30Nb obtained from previous studies [5,6] are also presented for comparison. The grinding ratios of the Ti–Nb–Cu alloys generally exhibited large variations (standard deviations). The ratios for 6Nb4Cu were higher than those for titanium at all grinding speeds, although the difference was not significant. The ratio for 6Nb4Cu at 1500 m/min was more than double that of Ti. The ratios for 18Nb2Cu and 24Nb1Cu were equal to or less than that of titanium at all grinding speeds. The ratio for 18Nb2Cu at 1000 m/min was significantly lower ( $p < 0.01$ ) than that of Ti. The 24Nb1Cu ratio at 750 m/min was significantly higher ( $p < 0.05$ ) than that of Ti.

### 3.4. Observation of Metal Chips, Wheels, and Ground Surfaces after Grinding

Figure 5 depicts the typical appearance of metal chips resulting from grinding at 750 and 1500 m/min. The alloy 6Nb4Cu exhibited curly chips post grinding that resembled those of titanium at 750 m/min. On the other hand, the metal chips of 18Nb2Cu and 24Nb1Cu, which had high grinding rates at 750 m/min, were lumpy and not curly. Abrasive grains shed from the grinding wheel were found to be mixed with chips resulting from 18Nb2Cu and 24Nb1Cu alloys. Although no quantitative analysis was performed, the metal chips from 18Nb2Cu and 24Nb1Cu appeared larger than those from 6Nb4Cu. At 1500 m/min, the metal chips from 6Nb4Cu were smaller and finer than those resulting from the 18Nb2Cu and 24Nb1Cu alloys.

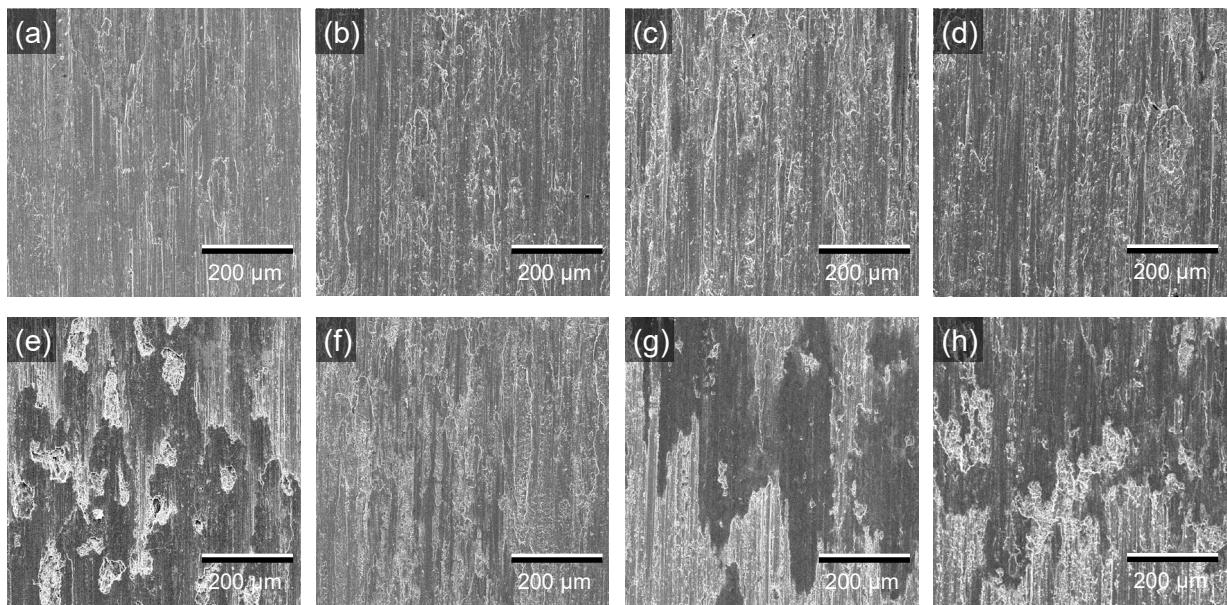


**Figure 4.** Grinding ratios for Ti–Nb–Cu alloys. At a particular grinding speed, identical letters indicate a statistically insignificant difference ( $p > 0.05$ ) between the grinding ratios for titanium and the alloy, whereas different letters indicate a statistically significant difference.



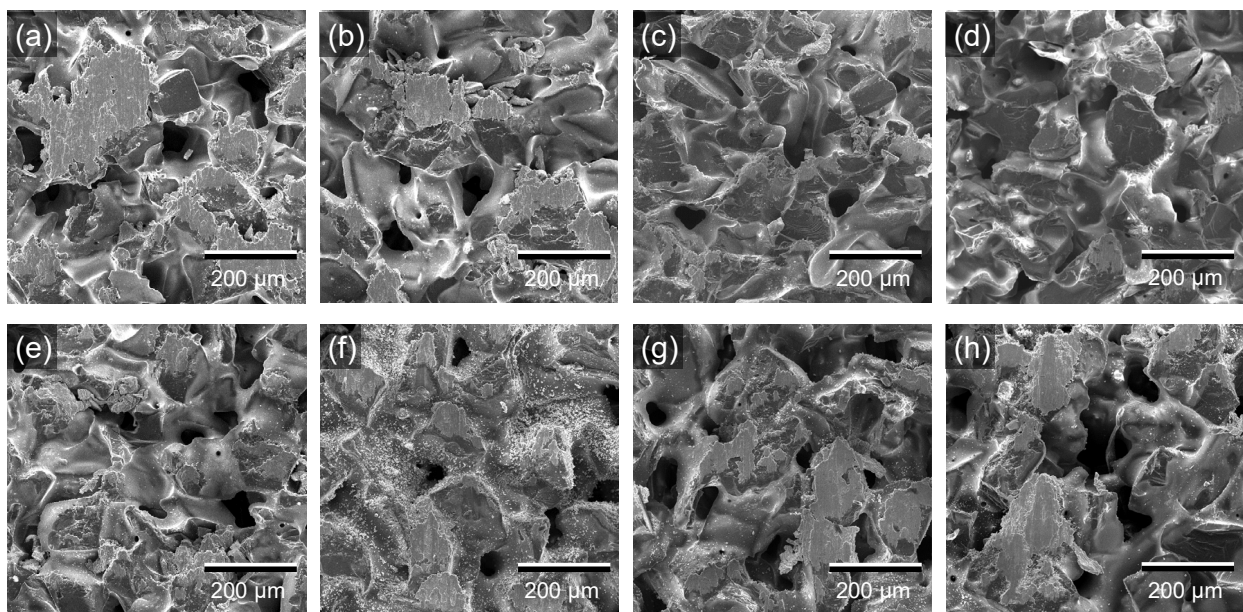
**Figure 5.** Metal chips resulting from grinding: (a) Ti; (b) 6Nb4Cu; (c) 18Nb2Cu; (d) 24Nb1Cu at 750 m/min; (e) Ti; (f) 6Nb4Cu; (g) 18Nb2Cu; (h) 24Nb1Cu at 1500 m/min. Arrows and alphabet indicate C: curly chips, L: lumpy (not curly) chips, A: abrasive grains.

Figure 6 depicts the ground surfaces of the alloys after grinding at 750 and 1500 m/min. After grinding at 750 m/min, the exposed surfaces of 18Nb2Cu and 24Nb1Cu alloys, which yielded large amounts of lumpy metal chips, did not exhibit any remarkable differences from that of 6Nb4Cu. At 1500 m/min, a significant difference was observed in the exposed surfaces after grinding. A grinding burn (discoloration of the surface caused by the heat generated during grinding) was observed on the exposed surfaces of Ti, 18Nb2Cu, and 24Nb1Cu. No obvious grinding burns were observed on the surface of 6Nb4Cu. In the qualitative analysis using EDS, oxygen was detected in addition to the alloy-component elements in the grinding-burn areas.



**Figure 6.** Exposed metal surfaces after grinding: (a) Ti; (b) 6Nb4Cu; (c) 18Nb2Cu; (d) 24Nb1Cu at 750 m/min; (e) Ti; (f) 6Nb4Cu; (g) 18Nb2Cu; (h) 24Nb1Cu at 1500 m/min.

The electron micrographs of the wheel surfaces after grinding are depicted in Figure 7. An adhesion of the metal-alloy material to the wheel surface (loading) was observed. At a grinding speed of 750 m/min, the wheels used to grind 18Nb2Cu and 24Nb1Cu were not significantly loaded. However, excessive loadings were observed on the wheels for the aforementioned alloys at 1500 m/min. Fine powdery material remained on the wheel surfaces that were used to grind 6Nb4Cu at 1500 m/min. Furthermore, qualitative examination using EDS confirmed the presence of titanium, niobium, and copper in the powder.



**Figure 7.** Wheel surfaces after grinding: (a) Ti; (b) 6Nb4Cu; (c) 18Nb2Cu; (d) 24Nb1Cu at 750 m/min; (e) Ti; (f) 6Nb4Cu; (g) 18Nb2Cu; (h) 24Nb1Cu at 1500 m/min.

## 4. Discussion

### 4.1. Alloy Phases and Hardness

In a previous study [13], the alloys 6Nb4Cu, 18Nb2Cu, and 24Nb1Cu were prepared under conditions identical to those in the current study; the microstructures of these alloys can be found in that study [13]. XRD analysis indicated that the alloy phases of 6Nb4Cu were  $\alpha + \text{Ti}_2\text{Cu}$ . A previous study on the mechanical properties and microstructures of Ti–Nb–Cu alloys demonstrated that the 6Nb4Cu alloy exhibited a single  $\alpha$  phase [13]. The bulk composition of 6Nb4Cu was found to be located at the boundary between the single  $\alpha$  phase and  $\alpha + \text{Ti}_2\text{Cu}$  phase in the Ti–Nb–Ti<sub>2</sub>Cu pseudo-ternary phase diagram for dental casting at room temperature, a diagram that we based on a previous study [16]. The precipitation of  $\text{Ti}_2\text{Cu}$  depends on the cooling rate of the casting [17,18]. The hardness of 6Nb4Cu (260) was found to be almost equal to that obtained in a previous study (256) [13]. Only trace amounts of the  $\text{Ti}_2\text{Cu}$  intermetallic compounds may have been precipitated; thus, no effect on the mechanical properties of the alloy was observed in this study. Minute amounts of fine  $\text{Ti}_2\text{Cu}$  may have been dispersed within the microstructure of the alloy, similar to Ti-5%Cu alloy casting [15]. The phases of the 18Nb2Cu alloy were  $\alpha + \beta$ , which is similar to the results of a previous study [13]. Based on the intensity of the peak in the XRD pattern, the structure of 18Nb2Cu was found to comprise a precipitated  $\alpha$  phase in the  $\beta$  phase (mostly  $\alpha$ ). The hardness of 18Nb2Cu (328) was found to be exactly equal to that reported in a previous study (328) [13]. The phases of the 24Nb1Cu alloy were found to be  $\beta + \alpha'' + \omega$ . A previous study on the mechanical properties and microstructures of Ti–Nb–Cu alloys revealed that the 24Nb1Cu alloy exhibited  $\beta + \alpha$  (near  $\beta$ ) phases [13]. A peak, likely related to the  $\omega$  phase, was found to exist at approximately 80°. However, because only one such peak was observed, the presence of the  $\omega$  phase could not be confirmed. This study confirmed the presence of the  $\omega$  phase based on the existence of four peaks. The  $\alpha''$  and  $\omega$  phases are metastable phases that appear when the cooling rate is sufficiently high during the transformation of  $\beta \rightarrow \alpha$  [19,20]. Although the cooling rate in this study is unknown, it may have been higher than that in the previous study. The hardness of the 24Nb1Cu alloy (377) was significantly higher than that of the other Ti–Nb–Cu alloys and comparable to that of Ti-30%Nb (375), whose alloy phases were  $\beta + \omega$  [6]. Thus, the high hardness value could have resulted from the precipitation of hard and brittle  $\omega$  phases [21].

Because the alloy phases and hardness of each composition closely matched those of a previous study [13], other mechanical properties such as strength and elongation are expected to be similar. The grindability, which was the focus of this study, is discussed in the next section in concurrence with mechanical properties, such as strength and elongation.

### 4.2. Grindability

The grinding rate and ratio of 6Nb4Cu increased as the grinding speed increased. At 1500 m/min, both parameters were almost double those of Ti. It was established that grinding at a high speed shortened the machining time of the 6Nb4Cu alloy and improved the tool life. It is generally known that a material with a good grindability has fine metal chips and, therefore, a good chip controllability [22]. Miniaturization of metal chips is a factor found to improve the grindability of 6Nb4Cu at high speed. The metal chips of 6Nb4Cu became finer during high-speed grinding as the long curly metal chips that were prominent during low-speed grinding became hardly visible. A powdery remnant of the metal was found on the wheels after high-speed grinding. This phenomenon was also observed in Ti-20%Ag and Ti-5%Cu alloys, which demonstrated good grindability [5]. Similarly, as in the case of the Ti-5%Cu alloy, fine  $\text{Ti}_2\text{Cu}$ , which acts as a free-machining inclusion, was precipitated. The presence of a precipitate and decreased elongation improved the grindability. The grinding rate and ratio of Ti-5%Nb, for which the amount of Nb added was close to that of 6Nb4Cu, were lower than those of titanium during high-speed grinding [5]. Therefore, it seems that Cu, rather than Nb, contributes to the improvement in grindability at high speeds. Moreover, 6Nb4Cu did not exhibit an

obvious grinding burn at high speeds in titanium and other Ti–Nb–Cu alloys. Therefore, the alloy 6Nb4Cu was concluded to demonstrate a good grindability.

The grinding rates of 18Nb2Cu, which had the highest tensile strength among the Ti–Nb–Cu alloys in this study, were higher (more than double) than those of titanium at medium grinding speeds of 750 and 1000 m/min. The grinding rate of the 18Nb2Cu alloy was significantly higher than that of titanium at a speed of 1000 m/min. Notably, its grinding ratio was smaller than that of titanium. The abrasive grains of the grinding wheel were also found to be mixed with the metal chips from the 18Nb2Cu alloy at 750 m/min. However, after grinding, the wheel did not present a significant amount of metal particles adhered to its surface. These observations imply that as the grinding rate increases, the grinding ratio decreases because of an active “self-sharpening” action. The alloy 18Nb2Cu has the advantage of a short processing time, although tool wear is high during medium-speed grinding. However, the grinding rates of Ti-15%Nb and Ti-20%Nb alloys, which are close to 18Nb2Cu in terms of the amount of Nb present, were highest at a grinding speed of 1000 m/min, but the difference between these rates and that of titanium was not significant [5]. No intermetallic compound precipitates were found in 18Nb2Cu or any other Ti–Nb alloy studied. In the alloy 18Nb2Cu, traces of Cu solid dissolved in  $\alpha/\beta$  titanium probably contributed to the improved grindability. The loading of the grinding wheels was observed at high speeds. The loading reduces the grinding rates and raises the surface temperature of the metal surface being ground, leading to burns. Grinding burn is a phenomenon in which the ground metal surface reacts with oxygen to form an oxide film due to the heat of grinding, and the color changes depending on the thickness of the oxide film. This phenomenon was observed during the grinding test of Ti–Au and Ti–Zr alloys, whose grindability did not improve [7,9].

For low-speed grinding, the grinding rate of 24Nb1Cu was higher than that of titanium. The grinding rate of 24Nb1Cu at 750 m/min was the highest value recorded in this study, four times that of titanium at the same speed. The grinding rate of 24Nb1Cu was higher than that of Ti-30%Nb, which is the basic baseline composition for all alloys designed in this study. However, as with 18Nb2Cu, the grinding ratio of 24Nb1Cu was lower than that of titanium. Nb is considered to improve the grinding rate of titanium but not its grinding ratio. Thus, Nb shortens the time required for machining but increases the wear of the machining tools. The appearance of metal chips and the wheel after grinding 24Nb1Cu was similar to that of 18Nb2Cu. It is postulated that the self-sharpening action of the wheel causes frequent exposure of a fresh surface of the wheel, thereby increasing the grinding rate while conversely lowering the grinding ratio of 18Nb2Cu and 24Nb1Cu at low speed. A factor that significantly improved the grindability of 24Nb1Cu was the precipitation of  $\omega$ , similar to that of Ti-30%Nb. It is well known that the body-centered-cubic-structured  $\beta$  is easily deformed and exhibits a good elongation, whereas the hexagonal-structured  $\omega$  is brittle and difficult to deform [21]. The  $\omega$  phase, which functions as a free machining inclusion, improves the grindability of 24Nb1Cu at low speed. The alloy Ti-25%Nb, which is close to 24Nb1Cu in terms of the amount of Nb added, primarily includes an  $\alpha''$  phase [5]. The  $\beta$  and  $\omega$  phases could not be confirmed in their structures. Cu was found to act like a  $\beta$ -stabilizing element for titanium [23]. This lowered the  $\beta \rightarrow \alpha$  transformation temperature ( $M_s$  temperature) and made it easier to retain the  $\beta$  phase at room temperature. Therefore, the possibility of a metastable phase  $\omega$  appearing in the alloy phase structure increased. Although only 1%Cu was added, it enhanced the appearance of the  $\omega$  phase. During high-speed grinding, the grinding rate of 24Nb1Cu decreased, similar to that of 18Nb2Cu, causing grinding burns on the exposed surface. The reason for the absence of active self-sharpening action in high-speed grinding remains unknown.

The grindability of the Ti–Nb–Cu alloys, examined in this study, was better than that of titanium. Each alloy exhibited a good grindability at different speeds. These alloys exhibited better grindability than the base binary alloys. Grinding is a process of cutting with abrasive grains of random shape and has a self-sharpening action, and cutting is the process of using a sharp edge of a certain shape to remove a substance but with no

self-sharpening action. Both processes remove unnecessary parts of the bulk material to obtain the required shape and dimensions. Machinability can be predicted, to a certain extent, from Grindability. For example, Ti–Ag alloys have been found to demonstrate a good grindability and machinability [24,25]. Therefore, Ti–Nb–Cu alloys are promising candidates for use as dental titanium alloys subjected to CAD/CAM. Our future work will involve investigating the machinability of Ti–Nb–Cu alloys with a milling machine.

## 5. Conclusions

High-strength Ti–Nb–Cu alloys were developed and investigated for their grindability. Consequently, the grinding rates for the 6Nb4Cu, 18Nb2Cu, and 24Nb1Cu alloys were found to significantly exceed that of titanium under high-, medium-, and low-speed grinding, respectively. In addition, 6Nb4Cu was found to exhibit an excellent grinding ratio. Thus, the Ti–Nb–Cu alloys developed in this study demonstrated favorable application potential as dental titanium alloys that can be subjected to CAD/CAM processing technologies.

**Author Contributions:** Conceptualization, M.T.; investigation, M.T.; data curation, M.T.; funding acquisition, M.T.; writing—original draft preparation, M.T.; formal analysis, M.K.; methodology, M.K.; validation, M.K. and Y.T.; writing—review and editing, M.K. and Y.T. All authors have read and agreed to the published version of the manuscript.

**Funding:** This study was partially supported by JSPS KAKENHI, grant number JP21K09930.

**Data Availability Statement:** The authors confirm that the data supporting the findings of this study are available within the article.

**Acknowledgments:** The authors acknowledge the assistance of Mary Wambui (KANYI) in proof-reading and editing the English version.

**Conflicts of Interest:** The authors declare no conflict of interest.

## References

1. Chandler, H.E. Machining of Reactive Metals. In *Machining*; ASM Handbook, ASM Handbook Committee; ASM International: Materials Park, OH, USA, 1989; Volume 16, pp. 844–857. [[CrossRef](#)]
2. Machado, A.R.; Wallbank, J. Machining of titanium and its alloys—a review. *Proc. Inst. Mech. Eng. Part B J. Eng. Manuf.* **1990**, *204*, 53–60. [[CrossRef](#)]
3. Ezugwu, E.O.; Wang, Z.M. Titanium alloys and their machinability—A review. *J. Mater. Process. Technol.* **1997**, *68*, 262–274. [[CrossRef](#)]
4. Okabe, T.; Ohkubo, C.; Watanabe, I.; Okuno, O.; Takada, Y. The present status of dental titanium casting. *JOM* **1998**, *50*, 24–29. [[CrossRef](#)]
5. Kikuchi, M.; Takahashi, M.; Okabe, T.; Okuno, O. Grindability of dental cast Ti–Ag and Ti–Cu Alloys. *Dent. Mater. J.* **2003**, *22*, 191–205. [[CrossRef](#)] [[PubMed](#)]
6. Kikuchi, M.; Takahashi, M.; Okuno, O. Mechanical properties and grindability of dental cast Ti–Nb alloys. *Dent. Mater. J.* **2003**, *22*, 328–342. [[CrossRef](#)] [[PubMed](#)]
7. Takahashi, M.; Kikuchi, M.; Okuno, O. Grindability of dental cast Ti–Zr alloys. *Mater. Trans.* **2009**, *50*, 859–863. [[CrossRef](#)]
8. Kikuchi, M.; Takahashi, M.; Sato, H.; Okuno, O.; Nunn, M.E.; Okabe, T. Grindability of cast Ti–Hf alloys. *J. Biomed. Mater. Res. B Appl. Biomater.* **2006**, *77*, 34–38. [[CrossRef](#)]
9. Takahashi, M.; Kikuchi, M.; Okuno, O. Mechanical properties and grindability of experimental Ti–Au alloys. *Dent. Mater. J.* **2004**, *23*, 203–210. [[CrossRef](#)]
10. Hsu, H.C.; Wu, S.C.; Chiang, T.Y.; Ho, W.F. Structure and grindability of dental Ti–Cr alloys. *J. Alloys Compd.* **2009**, *476*, 817–825. [[CrossRef](#)]
11. Lim, H.S.; Hwang, M.J.; Jeong, H.N.; Lee, W.Y.; Song, H.J.; Park, Y.J. Evaluation of surface mechanical properties and grindability of binary Ti alloys containing 5 wt% Al, Cr, Sn, and V. *Metals* **2017**, *7*, 487. [[CrossRef](#)]
12. Davis, J.R. (Ed.) *ASM Materials Engineering Dictionary*; ASM Press International: Materials Park, OH, USA, 1992; p. 175.
13. Takahashi, M.; Kikuchi, M.; Takada, Y. Mechanical properties and microstructures of dental cast Ti–6Nb–4Cu, Ti–18Nb–2Cu, and Ti–24Nb–1Cu alloys. *Dent. Mater. J.* **2016**, *35*, 564–570. [[CrossRef](#)] [[PubMed](#)]
14. *ISO 22674:2016*; Dentistry—Metallic Materials for Fixed and Removable Restorations and Appliances. ISO: Geneva, Switzerland, 2016; pp. 1–26. [[CrossRef](#)]

15. Takahashi, M.; Kikuchi, M.; Takada, Y.; Okuno, O. Mechanical properties and microstructures of dental cast Ti-Ag and Ti-Cu alloys. *Dent. Mater. J.* **2002**, *21*, 270–280. [[CrossRef](#)] [[PubMed](#)]
16. Sato, K.; Takahashi, M.; Takada, Y. Construction of Ti-Nb-Ti<sub>2</sub>Cu pseudo-ternary phase diagram. *Dent. Mater. J.* **2020**, *39*, 422–428. [[CrossRef](#)] [[PubMed](#)]
17. Holden, F.C.; Watts, A.A.; Ogden, H.R.; Jaffee, R.I. Heat treatment and mechanical properties of Ti-Cu alloys. *JOM* **1955**, *7*, 117–125. [[CrossRef](#)]
18. Taguchi, O.; Iijima, Y. Diffusion of copper, silver and gold in  $\alpha$ -titanium. *Philos. Mag. A* **1995**, *72*, 1649–1655. [[CrossRef](#)]
19. Collings, E.W.; Water, J.L.; Jackson, M.R.; Sims, C.T. (Eds.) *Introduction to Titanium Alloy Design, Alloying*; ASM International: Metals Park, OH, USA, 1988; pp. 257–370.
20. Murray, J.L. *The Nb-Ti (Niobium–Titanium) System, Phase Diagrams of Binary Titanium Alloys*; ASM International: Metals Park, OH, USA, 1990; pp. 188–194.
21. Hanada, S.; Ozeki, M.; Izumi, O. Deformation characteristics in  $\beta$  phase Ti-Nb alloys. *Metall. Trans. A* **1985**, *16*, 789–795. [[CrossRef](#)]
22. López de lacalle, L.N.; Pérez, J.; Llorente, J.I.; Sánchez, J.A. Advanced cutting conditions for the milling of aeronautical alloys. *J. Mater. Process. Technol.* **2000**, *100*, 1–11. [[CrossRef](#)]
23. Okamoto, H.; Massalski, T.B. *Binary Alloy Phase Diagrams*, 2nd ed.; Okamoto, H., Schlesinger, M.E., Mueller, E.M., Eds.; ASM International: Materials Park, OH, USA, 1990; Volume 2, p. 12.
24. Kikuchi, M.; Takahashi, M.; Okuno, O. Machinability of experimental Ti-Ag alloys. *Dent. Mater. J.* **2008**, *27*, 216–220. [[CrossRef](#)] [[PubMed](#)]
25. Inagaki, R.; Kikuchi, M.; Takahashi, M.; Takada, Y.; Sasaki, K. Machinability of an experimental Ti-Ag alloy in terms of tool life in a dental CAD/CAM system. *Dent. Mater. J.* **2015**, *34*, 679–685. [[CrossRef](#)]